



Published in final edited form as:

Dev Biol. 2017 September 01; 429(1): 44–55. doi:10.1016/j.ydbio.2017.07.011.

***Irx1* regulates dental outer enamel epithelial and lung alveolar type II epithelial differentiation**

Wenjie Yu^a, Xiao Li^b, Steven Eliason^a, Miguel Romero-Bustillos^c, Ryan J. Ries^a, Huojun Cao^c, and Brad A. Amendt^{a,c,*}

^aDepartment of Anatomy and Cell Biology, and the Craniofacial Anomalies Research Center, Carver College of Medicine, The University of Iowa, Iowa City, IA 52242, USA

^bDepartment of Cellular and Molecular Medicine, University of California, San Diego, CA, USA

^cIowa Institute for Oral Health Research, College of Dentistry, The University of Iowa, Iowa City, IA 52242, USA

Abstract

The *Iroquois* genes (*Irx*) appear to regulate fundamental processes that lead to cell proliferation, differentiation, and maturation during development. In this report, the *Iroquois homeobox 1* (*Irx1*) transcription factor was functionally disrupted using a *LacZ* insert and *LacZ* expression demonstrated stage-specific expression during embryogenesis. *Irx1* is highly expressed in the brain, lung, digits, kidney, testis and developing teeth. *Irx1* null mice are neonatal lethal and this lethality is due to pulmonary immaturity. *Irx1*^{-/-} mice show delayed lung maturation characterized by defective surfactant protein secretion and *Irx1* marks a population of SP-C expressing alveolar type II cells. *Irx1* is specifically expressed in the outer enamel epithelium (OEE), stellate reticulum (SR) and stratum intermedium (SI) layers of the developing tooth. *Irx1* mediates dental epithelial cell differentiation in the lower incisors resulting in delayed growth of the lower incisors. *Irx1* is specifically and temporally expressed during developmental stages and we have focused on lung and dental development in this report. *Irx1*⁺ cells are unique to the development of the incisor outer enamel epithelium, patterning of *Lef-1*⁺ and *Sox2*⁺ cells as well as a new marker for lung alveolar type II cells. Mechanistically, *Irx1* regulates *Foxj1* and *Sox9* to control cell differentiation during development.

Keywords

Irx1; Stem cells; Lung; Tooth; Cell differentiation; Alveolar type II cells

This is an open access article under the CC BY-NC-ND license (<http://creativecommons.org/licenses/by-nc-nd/4.0/>).

*Correspondence to: University of Iowa, Carver College of Medicine, and College of Dentistry, 1-675 BSB, 51 Newton Rd, Iowa City, IA 52242, USA. brad-amendt@uiowa.edu (B.A. Amendt).

Competing interests

The authors declare no competing or financial interests.

1. Introduction

Iroquois genes (*Irx*) encode a family of proteins with a homeobox domain and a characteristic Iroquois domain in the C terminal region. There are six members of the *Iroquois* family in mice and humans, which are located in two cognate clusters of three genes each (Houweling et al., 2001). It was reported that each cluster of *Iroquois* genes forms a three-dimensional structure to share the same enhancer, which dictates their similar expression patterns (Tena et al., 2011). *Irx3* and *Irx5* are crucial for cardiac morphogenesis and craniofacial development (Bonnard et al., 2012; Gaborit et al., 2012). *Irx3* is also related to determination of body mass and obesity (Smemo et al., 2014). *Irx1* is expressed in the brain, heart, lung, skin, and the craniofacial region, but its function is unclear. Several studies have indicated that *Irx1* is related to lung, brain, kidney and skeletal joint development, but limited research has been done to unveil its function and the cellular mechanisms through which it acts during development (Heliot et al., 2013; Smemo et al., 2014; Askary et al., 2015).

Tooth development, initiation, morphogenesis, and differentiation are controlled by a network of conserved signaling pathways and transcription factors (Thesleff and Tummers, 2008). Enamel formation is one of the most important events for tooth development, and occurs during the late stage of tooth morphogenesis. Inner enamel epithelial cells proliferate and differentiate into ameloblasts, which in turn synthesize enamel matrix proteins such as amelogenin and enamelin, which subsequently form the mineralized enamel layer (Zeichner-David et al., 1995). The maturation of ameloblasts is governed by extracellular signals, that regulate the activity of transcription factors to express genes required for enamel formation (Wang et al., 2004). The cell-cell interactions between ameloblasts, odontoblasts and the stratum intermedium are necessary for ameloblast maturation (Nakamura et al., 1991; Mitsiadis et al., 1995; Zeichner-David et al., 1995; Wang et al., 2004). Although the process and mechanism of amelogenesis is well studied, how extracellular signals from the enamel-free areas control the maturation of ameloblasts remains elusive (Wang et al., 2004).

Lung development originates from the endoderm and mesoderm during early development stages giving rise to branching morphogenesis, proximal-distal patterning of the epithelium and alveologenesis (Cardoso and Whitsett, 2008; Shi et al., 2009; Morrisey and Hogan, 2010; Ornitz and Yin, 2012; Hogan et al., 2014). While *Irx1* has been indicated in lung development the specific stages and cells expressing *Irx1* are not defined. The processes of branching and proximal-distal patterning of the lung epithelium are specific to *Sox2* and *Sox9* transcription factors (Chang et al., 2013; Rockich et al., 2013). Initial reports suggested that *Irx1* may play a role in lung development at these stages, however molecular mechanisms for *Irx1* function are not understood in alveologenesis and gene expression.

Our laboratory has generated RNA-seq data from multiple stages of craniofacial/tooth development in mice from E10.5 to P4 in an effort to identify new genes and pathways in craniofacial morphogenesis. Bioinformatics analyses identified *Irx1* expression at early stages of murine development. We generated the *Irx1* knockout mice (*Irx1*^{-/-}) to study the functional role of *Irx1* in development. We show detailed expression patterns of *Irx1* in both mouse embryos and adults. *Irx1* has a very unique expression pattern in dental development.

In bell stage teeth and adult teeth, *Irx1* is specific to the OEE, SI and SR cells. Identifying markers for these cells are limited and *Irx1* appears to mark these cells throughout development. *Foxj1* and *Sox9* control differentiation of these cell types during tooth development. We demonstrate that *Irx1* plays a role in regulating these genes and possibly as a cofactor for other transcription factors. *Irx1* null mice were neonatal lethal due to defects in lung development. Interestingly, in lung development, which relies on *FoxJ1* and *Sox9* expression, we speculate that *Irx1* expression in alveolar type II cells regulates these genes. In this article, we provide a study of *Irx1* in lung and tooth development.

2. Materials and methods

2.1. Mouse lines and embryonic staging

Mice are maintained in the animal facility of the University of Iowa. All experiments were approved by the Institutional Animal Care and Use Committee of the University of Iowa. The *Irx1* knockout ES cells were generated by the Knockout Mouse Project Repository (KOMP) in a C57BL/6 background. The genotyping primers for *Irx1* are listed below. WT-F: CCGAGGCACTGAGCTGTATC; WT-R: TGTTTCAGGTTGGAAGGGTTTCTA TG; KO-F: CTTCAAATTGTGTCTGAGAGC; KO-R: GTCTGTCCTAGCTTCC TCACTG. The *Irx1* mutant mice were made by blastocyst ES cell injection and chimeras were screened and mated to obtain *Irx1* genotypes. Injections and initial breedings were performed at the Texas A & M Health Science Center, Houston, TX. Embryos were staged by checking vaginal plug of the crossed females. The day with a vaginal plug was set as embryonic day (E) 0.5. For procedure of embryo harvesting, pregnant females were euthanized with CO₂ and followed with cervical dislocation. Then embryos were harvested and fixed immediately.

2.2. Cell culture and Lentivirus-based *Irx1* knockdown

Rat AEC2 (RLE-6TN, ATCC[®] CRL-2300[™]), HEK 293T (ATCC[®] CRL-11268[™]) and ET-16 oral epithelia cells (gift from Dr. Malcolm Snead, USC) were cultured in DMEM supplemented with 5% FBS, 5% BGS and penicillin/streptomycin at 37 °C with 5% CO₂. Lentiviruses were produced by transiently transfected scramble or knockdown constructs in pLKO.1-puro vector together with viral packaging vectors (psPAX2, pMD2G) into HEK 293T cells by calcium phosphate transfection. DMEM supernatant with lentiviruses was harvested 30 h post-transfection and directly used for infection. ET-16 cells were infected with lentiviruses for 48 h and then selected with 5 µg/ml of puromycin (Sigma P8833) for another 3 days before further analysis. Lentivirus-based scramble sequence (*shNC*): 5'-CCTAAGGTTAAGTCGCCCTCG-3'; *Irx1* knockdown sequence (*shIrx1*): 5'-CCACACAACGCCTGCTTATTA-3'.

2.3. Antibodies and reagents

The following antibodies were used for immunoblotting and immunostaining: anti-IRX1 (Sigma HPA043160, 1:100 – 1:300), anti-IRX1 (abcam ab98343, 1:200 – 1:500), anti-Lef-1 (Cell signaling #2230, 1:200), anti-Sox2 (R & D systems AF2018, 1:150 & D systems AF2018, 1:150), anti-SP-C (Santa Cruz sc-7706, 1:300), anti-BrdU (abcam ab6326, 1:1000), anti-CldU (Accurate chemical OBT0030, 1:250), anti-IdU (Roche 11170376001, 1:250). Secondary staining was performed using Alex Fluor488 donkey anti-mouse IgG (Invitrogen

A21202, 1:500), Alex Fluor594 donkey anti-mouse IgG (Invitrogen A21203, 1:500), Alex Fluor488 donkey anti-rabbit IgG (Invitrogen A21206, 1:500) DAPI (Invitrogen D1306, 1 µg/ml), Beta-gal (Promega V3941).

2.4. X-gal staining

Embryos and organs were isolated and pre-fixed with ice-cold fixative buffer (1×PBS with 1% formaldehyde, 0.2% glutaraldehyde and 0.02% NP40) for 2 h at 4 °C. Next, tissues were washed twice (20 min each) in washing buffer (1×PBS with 2 mM MgCl₂, 0.02% NP40 and 0.1% sodium deoxycholate) at room temperature. Tissues were then stained with X-gal (1 mg/ml X-gal, 5 mM K₃Fe(CN)₆ and 5 mM K₄Fe(CN)₆ in washing buffer) at room temperature overnight. Then they were washed in 1×PBS twice (20 min each) at room temperature and were fixed in 4% PFA overnight. After fixation, the tissues were washed with 1×PBS and imaged with a dissection microscopy in whole mount or after paraffin embedding and sectioning.

Tissue sections (4–6 µm) were taken and prepared with a standard de-paraffinization and hydration process, then stained with eosin or nuclear fast red solution (1 g/L nuclear fast red, 50 g/L Al₂[SO₄]₃·18H₂O).

2.5. Lung collection and processing

For embryonic stage lung processing, embryos were incubated on ice for 10 min and then the top half of embryos were washed with 1×PBS and fixed in 4% PFA. After fixation, the left lung was dissected and embedded in paraffin. For lung tissue RNA preparation, the left lung was collected before fixation and snap frozen before processing. For postnatal stage lungs, mice were perfused with 1×PBS at the right ventricle to clear the pulmonary vasculature. Then lungs were inflated with 1×PBS through the trachea and fixed in ice-cold 4% PFA.

2.6. Immunostaining and imaging

Embryos and tissues were harvested in fresh and washed with ice-cold 1×PBS once, then fixed with 4% PFA and washed with 1×PBS for 3 times to clear residual PFA. After fixation, embryos and tissues were kept in 70% ethanol and then taken through a standard dehydration and paraffin-embedding process. Sections were cut in 4–6 µm. After de-paraffinization and hydration, sections were treated with citrate buffer in 100 °C water bath for 20 min. For immunofluorescent staining, sections were blocked with donkey serum and incubated with proper primary antibodies overnight in 4 °C. Then sections were washed with 1×PBS, incubated with Alex Fluor488/594 secondary antibodies and stained with DAPI. For immunohistochemistry staining, sections were processed according to the manufacturer of the IHC kit (Abcam, ab64264). Images were captured by Zeiss 700 confocal microscopy or Nikon eclipse microscopy. The integrated density of fluorescent signals was calculated by using the ImageJ software. The length of the entire mandible and lower incisors (measured from the cervical loop to the tip of the lower incisor with the dental lamina) were measured in ImageJ software with the absolute value relative to scale bars in each image.

2.7. BrdU, CldU and IdU labeling

BrdU (Invitrogen, #00-0103), CldU (Sigma, #C6891) and IdU (Sigma, #17125) were delivered into pregnant females by intraperitoneal injection at different time points. Following the standard immunostaining process, sections were treated with 2 M HCl for 1 h and neutralized with 1×PBS. Detailed IdU/CldU labeling processes could be found in our previous paper (Sun et al., 2016).

2.8. Quantitative RT-PCR

Total RNAs were isolated from tissues and cells by standard RNA preparation protocols. cDNAs were made by TaKaRa kit (TaKaRa, RR036A) and followed with standard quantitative RT-PCR. PCR primers are listed in Table 2.

3. Results

3.1. Generation of *Irx1* knockout mice

Gene expression analysis of dental epithelial and mesenchymal cells in neonatal mice showed that several hundred genes had significantly higher expression in dental epithelial cells than mesenchymal cells (data not shown). *Irx1* was one of these novel genes, with an expression level that is higher in dental epithelial cells compared to mesenchymal cells.

In order to unveil the function of *Irx1* during craniofacial/dental development we disrupted the *Irx1* gene in mice. The *Irx1* coding region was replaced with an exogenous *LacZ* reporter gene (Fig. 1A), which allowed us to detect the expression pattern of *Irx1* during development. Two pairs of genotyping primers (probes) were designed as shown in Fig. 1A. PCR results from tail genomic DNA showed *Irx1*^{+/+} mice had a 100 bp band, while *Irx1*^{-/-} mice only had a 400 bp band (Fig. 1B). To demonstrate that *Irx1* was truly ablated in *Irx1*^{-/-} mice, we probed for the presence of *Irx1* mRNA and protein from both *Irx1*^{+/+} and *Irx1*^{-/-} tissues. Quantitative RT-PCR and Western blot results showed that *Irx1* was successfully deleted in *Irx1*^{-/-} mice (Fig. 1C, D).

3.2. *Irx1* expression patterns in early murine development

Embryos from E10.5 to E13.5 were harvested and subjected to whole-mount X-gal staining. X-gal staining results in *Irx1*^{+/-} whole embryos showed that *Irx1* is highly expressed in the brain, somites, lung, kidney, reproductive organs, eye, and limb buds and digits (Fig. 2A–D), which is consistent with previous studies (Becker et al., 2001; Houweling et al., 2001; Diaz-Hernandez et al., 2013; Heliot et al., 2013). In order to examine whether *Irx1* was still expressed in these organs at adult stages, organs from postnatal day (P) 30 adult *Irx1*^{+/-} mice were collected and stained with X-gal. *Irx1* is expressed in mid-brain, lung, kidney, skin, testis and epididymis (Fig. 2E–H). H & E staining of sections from these tissues are shown in Fig. 2I to L. *Irx1* is expressed in the skin hair follicle, alveoli of the lung epithelium, intermediate tubules in the kidney, and spermatocytes in the testis (Fig. 2I–L).

In teeth, *Irx1* is expressed in the entire dental epithelial cell population including the vestibular lamina (VL) at the early stages of tooth development, and its expression is narrowed to the dental epithelium at later stages of incisor development (Fig. 3A, B). In late

bell stage teeth, *Irx1* is only expressed in three specific cell layers, namely, outer enamel epithelium (OEE), stratum intermedium (SI) and stellate reticulum (SR) (Fig. 3C, D). This highly specific expression pattern was confirmed in adult teeth by X-gal staining (Fig. 3E).

3.3. *Irx1* ablation leads to neonatal lethality and lung developmental defects

We analyzed the genotypes of the offspring of *Irx1*^{+/-} intercrosses. At P0, the *Irx1*^{+/+} and *Irx1*^{+/-} mice had a birth ratio of 1:2, and no *Irx1*^{-/-} mice were found (Table 1). At early embryonic stages, *Irx1*^{-/-} embryos were found with normal Mendelian frequency (Table 1). With careful analysis, we found *Irx1*^{-/-} pups were born with normal Mendelian frequency, but died within several hours of delivery (Table 1). These *Irx1*^{-/-} mice had abnormal thoracic contractions, had labored breathing and difficulties with respiration (video not shown). In addition, *Irx1*^{-/-} pups had a purple body color and showed no evidence of milk ingestion, which is a phenotype commonly associated with respiratory failure or cleft palate (Turgeon and Meloche, 2009) (Fig. 4A). Coronal sections of P0 *Irx1*^{-/-} mouse heads were performed for histological analysis, and we found no evidence of cleft palate defects (data not shown). The lungs from *Irx1*^{-/-} pups were smaller compared to the lungs from *Irx1*^{+/+} pups, but the total body weight of *Irx1*^{-/-} pups were not significantly decreased (Fig. 4B, C). Histological analysis of the left lung from E16.5 embryos showed no significant difference in lung structure, however the *Irx1*^{-/-} lungs were smaller in size (Fig. 4D). Histological analysis at E18.5 showed that the lungs from *Irx1*^{-/-} embryos had more saccular space, and much of the saccular space was not well formed. Interestingly, histological analysis at P0 showed opposite results. The lungs from *Irx1*^{+/+} pups had more saccular space compared to the lungs from *Irx1*^{-/-} pups, in contrast to our findings at E18.5. Since the lungs used for histological analysis were not inflated, the saccular space in *Irx1*^{-/-} lungs may have collapsed after birth (Fig. 4E).

3.4. *Irx1* is expressed in alveolar type II epithelial cells and regulates expression of surfactant proteins

Because *Irx1* is expressed in a specific cell population in the lung, we asked whether *Irx1* was expressed in the alveolar type II epithelium (AEC2). We performed double immunostaining of *Irx1* and SP-C, a surfactant protein that marks AEC2 cells. Specifically, all the cells stained with *Irx1* were also stained with SP-C, although we did find a small population of cells that were only stained with SP-C (Fig. 5A, white arrow, SP-C; yellow arrows, both, in merged panel). We confirmed this result in AEC2 cell lines from rat. Immunostaining of *Irx1* in cultured type II cells from the rat showed that most type II cells had *Irx1* positive signals in the nucleus (Fig. 5B). To determine whether *Irx1* is required for AEC2 cells to function normally, we examined surfactant protein expression in lungs from both *Irx1*^{+/+} and *Irx1*^{-/-} mice. Immunostaining of SP-C at P0 stages showed that SP-C protein levels were down-regulated in *Irx1*^{-/-} lungs (bottom panels) (Fig. 5C, D). Quantitative RT-PCR analysis of the mRNA levels of surfactant proteins showed that *Sftpa1*, *Sftpc* and *Sftpd* were significantly down-regulated in E18.5 *Irx1*^{-/-} lungs (Fig. 5E).

3.5. Incisor and molar reduced growth is associated with cell differentiation in *Irx1*^{-/-} mice

With the unique expression pattern of *Irx1* in teeth, we asked whether *Irx1* loss-of-function would affect tooth development. Immunostaining of *Irx1* confirmed that *Irx1* was ablated in

Irx1 knockout mice (Fig. 3B, D), making it an ideal model to determine the role of *Irx1* in OEE, SR and SI cellular function. In E13.5 *Irx1*^{-/-} embryos, the lower incisors showed reduced cell differentiation (poorly polarized dental epithelium) (Fig. 6A). At later stages, we sectioned the entire heads of E18.5 and P0 *Irx1*^{+/+} and *Irx1*^{-/-} mice, we did not observe any difference about the size of the entire head and mandible between *Irx1*^{+/+} and *Irx1*^{-/-} mice (data not shown). We only observed molars and lower incisor growth was reduced in *Irx1*^{-/-} embryos compared to molars and lower incisors from *Irx1*^{+/+} embryos (Fig. 6B,C,D). Lower incisors in *Irx1*^{-/-} embryos and neonates were approximately 85% the length of the lower incisors from *Irx1*^{+/+} embryos and neonates, indicating that *Irx1* regulated later stages of tooth morphogenesis.

We next tested whether cell proliferation versus cell differentiation was down-regulated in *Irx1*^{-/-} teeth and if this could explain the smaller tooth phenotype. BrdU incorporation assays were performed in E18.5 lower incisors. In E18.5 lower incisors, the inner enamel epithelial (IEE) cells close to the cervical loop region were labeled with BrdU signals (Fig. 7A, blue arrows). In contrast, the outer enamel epithelial (OEE) cells, which express *Irx1*, were not labeled with BrdU in the *Irx1*^{-/-} embryos compared to WT (Fig. 7A, black arrows). In addition, there was not a significant difference between BrdU positive cells in the IEE cell layers when comparing the *Irx1*^{+/+} and *Irx1*^{-/-} lower incisors (Fig. 7B), indicating that cell proliferation is not significantly altered in *Irx1*^{-/-} teeth. We next asked whether cell differentiation was down-regulated in *Irx1*^{-/-} teeth. We performed 5-chloro-2-deoxyuridin (CIdU) and 5-iodo-2-deoxyuridin (IdU) pulse-chase experiments. CIdU and IdU were injected at different time points (pulse), and labeled cells were analyzed by double fluorescent staining (CIdU, 36 h; IdU, 2 h, see diagram). Cells retaining the CIdU label would have divided and migrated from the labial cervical loop (LaCL) region before cells retaining the IdU label. Recent cell proliferation in the LaCL is shown by cells retaining the IdU label. As expected, IdU+ cells (green) marked cells undergoing proliferation at the labial cervical loop region (P) (Fig. 7C). In contrast, CIdU+ cells (red) not only marked those cells, but also cells that differentiated from this region of the lower incisors (NP) (Fig. 7C). We analyzed the number of IdU+ cells and CIdU+ cells in the lower incisor epithelial layers. There were less CIdU+ cells at the proximal region (P region) of *Irx1*^{+/+} lower incisors compared to *Irx1*^{-/-} incisors and more CIdU+ cells at the distal regions (NP region) in *Irx1*^{+/+} lower incisors compared to *Irx1*^{-/-} lower incisors (Fig. 7D), indicating that CIdU+ cells remained in the LaCL region (P) in *Irx1*^{-/-} lower incisors and did not differentiate compared to *Irx1*^{+/+} lower incisors.

3.6. *Irx1* regulates the number and partitioning of Lef-1+ and Sox2+ cells during incisor development

While *Irx1* is expressed in the early dental epithelium and the dental placode, at later stages it is specifically expressed in the OEE, which was not a significant part of the cell populations labeled in the pulse-chase experiments (Fig. 7). Therefore, we hypothesized that decreased cell differentiation in the incisor was a secondary effect caused by defects in OEE cell differentiation. We have previously shown that Sox2 and Lef-1 contribute to distinct cell populations in the developing lower incisor (Zhao, Yu et al., 2016). Double fluorescent staining showed that Lef-1 and Sox2 are expressed in distinct cell populations of the lower

incisor (Fig. 8A, top panels). We asked whether these distinct populations of cells were affected by ablating *Irx1* expression in the incisor. We examined Lef-1+ and Sox2+ cell distribution in cap stage lower incisors of *Irx1*^{+/+} and *Irx1*^{-/-} embryos. Interestingly, both Lef-1+ and Sox2+ cell distribution within the dental epithelium were altered. In WT (*Irx1*^{+/+}) cap stage teeth, Sox2+ cells were localized to the labial cervical loop region, but Sox2+ cells were localized not only in the labial cervical loop region, but also in a lingual region close to the oral epithelium in *Irx1*^{-/-} embryos (Fig. 8A, second panel, white asterix), which is a region that expresses *Irx1* (Fig. 3B). Furthermore, Lef-1 expression is reduced in the surrounding lingual dental mesenchyme in the *Irx1*^{-/-} embryos, adjacent to the region of increased Sox2+ epithelial cells (Fig. 8A, second panel, yellow asterix). In late bell stage incisors (E18.5), *Irx1* is expressed in the OEE cells adjacent and separate from Sox2+ cells in the LaCL (Fig. 8B). X-gal staining of *Irx1*^{+/+} and *Irx1*^{-/-} lower incisors demonstrate less X-gal positive cells in the OEE cell layer of *Irx1*^{-/-} lower incisors, indicating that the dental stem cell to OEE differentiation pathway was down-regulated in part by the absence of functional *Irx1* (Fig. 8C). In support of this both the OEE and SI cell layers are underdeveloped as are the preameloblasts (AM) of the IEE and odontoblasts (OD).

3.7. *Irx1* regulates *Foxj1* and *Sox9* expression

In order to characterize the regulatory role of *Irx1* during tooth development, we isolated total RNA from E14.5 *Irx1*^{+/+} and *Irx1*^{-/-} maxillary and mandibular tissues to perform RNA-seq analysis. RNA-seq results showed approximately 300 genes were down-regulated and 70 genes were upregulated (Fig. 9A), suggesting that *Irx1* predominantly acts as a transcriptional activator during tooth development. The top functional gene cluster among the down-regulated genes were those implicated in cell differentiation such as *Foxj1*, *Sox9*, *Lhx2*, *Foxa1* and *Sox5* (Fig. 9B). Among these gene clusters, *Foxj1* was down-regulated and of great interest to us, since our previous studies found that the *Foxj1* knockout mice displayed arrested OEE cell differentiation and reduced tooth growth (Venugopalan et al., 2011). In order to confirm the RNA-seq results, we performed quantitative RT-PCR analysis of *Foxj1* from P0 lower incisor tissues. The *Foxj1* transcript level was reduced 60% in *Irx1*^{-/-} lower incisors (Fig. 9C). We also confirmed this regulation in cultured cells by knocking down *Irx1* in ET-16 oral epithelial cells (Fig. 9D). Together, these results support the idea that *Irx1* plays an important role in regulating the expression of genes that are responsible for cell differentiation and reveals an especially important role for *Irx1* and these associated factors during tooth and lung morphogenesis. *Irx1* may also act as an important transcription co-factor through protein interactions facilitated by its Iro domain.

4. Discussion

In this article, we have shown that *Irx1* is specifically expressed in AEC2 and OEE cells. *Irx1* regulates alveolar progenitors and dental stem cell differentiation by regulating the expression of differentiation-related genes such as *Foxj1* (Fig. 9E). Ablation of *Irx1* in AEC2 cells disrupted surfactant protein secretion, which provides surfactant tension in the lung sacculus space for breathing. In preparation for normal breathing after birth, the lung is required to develop mature AEC1 and AEC2 cells during sacculation (Morrissey and Hogan, 2010, Desai et al., 2014). Our findings of *Irx1* in AEC2 cells provide a new candidate gene

to further study molecular mechanisms of lung development. We show that *Irx1* is expressed in AEC2 cell populations. It is reported that AEC2 cells are progenitor cells in the alveolar sacs, which are responsible for alveolar self-renewal and repair after injury (Barkauskas et al., 2013, Desai et al., 2014). *Irx1* could be a more specific marker for progenitor-like AEC2 cells compared to SP-C in adult lung. There are two possible functions of *Irx1* during alveologenesis: 1) *Irx1* regulates the transcription of surfactant proteins, and/or 2) *Irx1* regulates progenitor cells differentiation into mature AEC2 cells. The identification that *Irx1* positively regulates *Foxj1* and *Sox9* expression and negatively regulates *Sox2* expression suggests a role in the transition of progenitor cells toward mature AEC2 cells and the saccular phase. We are currently generating *Irx1-3ox/3ox* conditional knockout and *Irx1-Cre* animals to determine the detailed cellular and molecular mechanisms of *Irx1* during development.

We also demonstrated that *Irx1* was expressed in dental epithelial cells of the placode stage and bud stage teeth, and then limited to specific epithelial cell layers. Three cell types located labial to the ameloblasts, the outer enamel epithelium (OEE), stellate reticulum (SR) and stratum intermedium (SI) are reported to be associated with amelogenesis. In the *Msx2* knockout mouse, the structure of the stratum intermedium layer is disrupted, which impairs normal ameloblast function and enamel deposition (Satokata et al., 2000). *Irx1* appears to have a similar function, but its more specific expression in these cell types differentiates it from *Msx2*. However, ablation of *Irx1* is novel because of its specific expression in these cell types and as a unique marker for late stage OEE, and SI. The lack of *Irx1* in incisors leads to defective OEE cell differentiation in the lower incisors. As a result, IEE cell differentiation is down-regulated and tooth growth is reduced. *Irx1* ablation during early stages of tooth development appears to regulate the positioning of Sox2+ and Lef-1+ cell niches within the tooth germ. The increase in Sox2+ cells in the *Irx1*^{-/-} mice suggest that *Irx1* is regulating the positioning and/or boundary of Sox2+ cells during development. Interestingly, during normal development *Irx1* delineates a boundary between Sox2+ and *Irx1*+ cells in the OEE. While we do not provide evidence that *Irx1* directly inhibits Sox2 expression, we have preliminary data that indicates *Irx1* interacts with other proteins to down-regulate activation of Sox2 expression (data not shown). *Irx1* can directly interact with other factors to regulate their transcriptional activity and downstream targets. Our findings provide evidence that OEE, SR and SI cells are necessary for tooth development. Although these cells do not produce enamel and dentin to form the hard structures of the tooth, they are required for normal tooth formation. Preliminary data also suggests that *Irx1* marks cementoblasts cells in mice molars (data not shown).

In this report, we focused on the cell and tissue developmental activity of *Irx1* at the later stages of embryonic development, but the function of *Irx1* in early lung and tooth development is still elusive. *Irx1* is expressed very early during organogenesis, but the defects caused by *Irx1* ablation appeared to be mild. Considering *Irx1*, *Irx2*, and *Irx6* share the same enhancer and co-regulators, it is possible that gene redundancy plays a role in such circumstances. In order to further determine the detailed functions of *Irx1* during embryonic development, a double or triple knockout strategy could be a better way to determine the global functions of the *Iroquois* family.

Acknowledgments

This work was supported by funds from the University of Iowa Carver College of Medicine, University of Iowa College of Dentistry and National Institutes of Health, grant DE13941 and R90 DE024296-03. We thank William Shalot (Texas A & M Health Science Center, Houston, TX) for ES cell injections and mutant mouse development. We thank Dr. Malcolm Snead (USC, Los Angeles, CA) for the ET-16 oral epithelial cell line. We thank Drs. Hank Qi, John Engelhardt and David Meyerholz, (University of Iowa, Iowa City, IA) for reagents, helpful comments and ideas and all of the members of the Amendt laboratory for their help and comments.

References

- Askary A, Mork L, Paul S, He X, Izuhara AK, Gopalakrishnan S, Ichida JK, McMahon AP, Dabizljevic S, Dale R, Mariani FV, Crump JG. Iroquois proteins promote skeletal joint formation by maintaining chondrocytes in an immature state. *Dev Cell*. 2015; 35(3):358–365. [PubMed: 26555055]
- Barkauskas CE, Cronce MJ, Rackley CR, Bowie EJ, Keene DR, Stripp BR, Randell SH, Noble PW, Hogan BL. Type 2 alveolar cells are stem cells in adult lung. *J Clin Invest*. 2013; 123(7):3025–3036. [PubMed: 23921127]
- Becker MB, Zulch A, Bosse A, Gruss P. Irx1 and Irx2 expression in early lung development. *Mech Dev*. 2001; 106(1–2):155–158. [PubMed: 11472847]
- Bonnard C, Strobl AC, Shboul M, Lee H, Merriman B, Nelson SF, Ababneh OH, Uz E, Guran T, Kayserili H, Hamamy H, Reversade B. Mutations in IRX5 impair craniofacial development and germ cell migration via SDF1. *Nat Genet*. 2012; 44(6):709–713. [PubMed: 22581230]
- Cardoso WV, Whitsett JA. Resident cellular components of the lung: developmental aspects. *Proc Am Thorax Soc*. 2008; 5:767–771.
- Chang DR, Martinez Alanis D, Miller RK, Ji H, Akiyama H, McCrea PD, Chen J. Lung epithelial branching program antagonizes alveolar differentiation. *Proc Natl Acad Sci USA*. 2013; 110(45):18042–18051. [PubMed: 24058167]
- Desai TJ, Brownfield DG, Krasnow MA. Alveolar progenitor and stem cells in lung development, renewal and cancer. *Nature*. 2014; 507(7491):190–194. [PubMed: 24499815]
- Diaz-Hernandez ME, Bustamante M, Galvan-Hernandez CI, Chimal-Monroy J. Irx1 and Irx2 are coordinately expressed and regulated by retinoic acid, TGFbeta and FGF signaling during chick hindlimb development. *PLoS One*. 2013; 8(3):e58549. [PubMed: 23505533]
- Gaborit N, Sakuma R, Wylie JN, Kim KH, Zhang SS, Hui CC, Bruneau BG. Cooperative and antagonistic roles for Irx3 and Irx5 in cardiac morphogenesis and postnatal physiology. *Development*. 2012; 139(21):4007–4019. [PubMed: 22992950]
- Heliot C, Desgrange A, Buisson I, Prunskaitė-Hyyryläinen R, Shan J, Vainio S, Umbhauer M, Cereghini S. HNF1B controls proximal-intermediate nephron segment identity in vertebrates by regulating Notch signalling components and Irx1/2. *Development*. 2013; 140(4):873–885. [PubMed: 23362348]
- Hogan BL, Barkauskas CE, Chapman HA, Epstein JA, Jain R, Hsia CC, Niklason L, Calle E, Le A, Randell SH, Rock J, Snitow M, Krummel M, Stripp BR, Vu T, White ES, Whitsett JA, Morrisey EE. Repair and regeneration of the respiratory system: complexity, plasticity, and mechanisms of lung stem cell function. *Cell Stem Cell*. 2014; 15(2):123–138. [PubMed: 25105578]
- Houweling AC, Dildrop R, Peters T, Mummenhoff J, Moorman AF, Ruther U, Christoffels VM. Gene and cluster-specific expression of the Iroquois family members during mouse development. *Mech Dev*. 2001; 107(1–2):169–174. [PubMed: 11520674]
- Mitsiadis TA, Lardelli M, Lendahl U, Thesleff I. Expression of Notch 1, 2 and 3 is regulated by epithelial-mesenchymal interactions and retinoic acid in the developing mouse tooth and associated with determination of ameloblast cell fate. *J Cell Biol*. 1995; 130(2):407–418. [PubMed: 7615640]
- Morrisey EE, Hogan BL. Preparing for the first breath: genetic and cellular mechanisms in lung development. *Dev Cell*. 2010; 18(1):8–23. [PubMed: 20152174]

- Nakamura M, Bringas P Jr, Slavkin HC. Inner enamel epithelia synthesize and secrete enamel proteins during mouse molar occlusal “enamel-free area” development. *J Craniofac Genet Dev Biol.* 1991; 11(2):96–104. [PubMed: 1869617]
- Ornitz DM, Yin Y. Signaling networks regulating development of the lower respiratory tract. *Cold Spring Harb Perspect Biol.* 2012; 4(5)
- Rockich BE, Hrycaj SM, Shih HP, Nagy MS, Ferguson MA, Kopp JL, Sander M, Wellik DM, Spence JR. *Sox9* plays multiple roles in the lung epithelium during branching morphogenesis. *Proc Natl Acad Sci USA.* 2013; 110(47):E4456–E4464. [PubMed: 24191021]
- Satokata I, Ma L, Ohshima H, Bei M, Woo I, Nishizawa K, Maeda T, Takano Y, Uchiyama M, Heaney S, Peters H, Tang Z, Maxson R, Maas R. *Msx2* deficiency in mice causes pleiotropic defects in bone growth and ectodermal organ formation. *Nat Genet.* 2000; 24(4):391–395. [PubMed: 10742104]
- Shi W, Xu J, Warburton D. Development, repair and fibrosis: what is common and why it matters. *Respirology.* 2009; 14(5):656–665. [PubMed: 19659647]
- Smemo S, Tena JJ, Kim KH, Gamazon ER, Sakabe NJ, Gomez-Marin C, Aneas I, Credidio FL, Sobreira DR, Wasserman NF, Lee JH, Puviindran V, Tam D, Shen M, Son JE, Vakili NA, Sung HK, Naranjo S, Acemel RD, Manzanares M, Nagy A, Cox NJ, Hui CC, Gomez-Skarmeta JL, Nobrega MA. Obesity-associated variants within *FTO* form long-range functional connections with *IRX3*. *Nature.* 2014; 507(7492):371–375. [PubMed: 24646999]
- Sun Z, Yu W, Sanz Navarro M, Sweat M, Eliason S, Sharp T, Liu H, Seidel K, Zhang L, Moreno M, Lynch T, Holton NE, Rogers L, Neff T, Goodheart MJ, Michon F, Klein OD, Chai Y, Dupuy A, Engelhardt JF, Chen Z, Amendt BA. *Sox2* and *Lef-1* interact with *Pitx2* to regulate incisor development and stem cell renewal. *Development.* 2016; 143(22):4115–4126. [PubMed: 27660324]
- Tena JJ, Alonso ME, de la Calle-Mustienes E, Splinter E, de Laat W, Manzanares M, Gomez-Skarmeta JL. An evolutionarily conserved three-dimensional structure in the vertebrate *Irxf* clusters facilitates enhancer sharing and coregulation. *Nat Commun.* 2011; 2:310. [PubMed: 21556064]
- Thesleff I, Tummers M. *Tooth Organogenesis and Regeneration.* StemBook; Cambridge (MA): 2008.
- Turgeon B, Meloche S. Interpreting neonatal lethal phenotypes in mouse mutants: insights into gene function and human diseases. *Physiol Rev.* 2009; 89(1):1–26. [PubMed: 19126753]
- Venugopalan SR, Li X, Amen MA, Florez S, Gutierrez D, Cao H, Wang J, Amendt BA. Hierarchical interactions of homeodomain and forkhead transcription factors in regulating odontogenic gene expression. *J Biol Chem.* 2011; 286(24):21372–21383. [PubMed: 21504905]
- Wang XP, Suomalainen M, Jorgez CJ, Matzuk MM, Werner S, Thesleff I. Follistatin regulates enamel patterning in mouse incisors by asymmetrically inhibiting BMP signaling and ameloblast differentiation. *Dev Cell.* 2004; 7(5):719–730. [PubMed: 15525533]
- Zeichner-David M, Diekwisch T, Fincham A, Lau E, MacDougall M, Moradian-Oldak J, Simmer J, Snead M, Slavkin HC. Control of ameloblast differentiation. *Int J Dev Biol.* 1995; 39(1):69–92. [PubMed: 7626423]

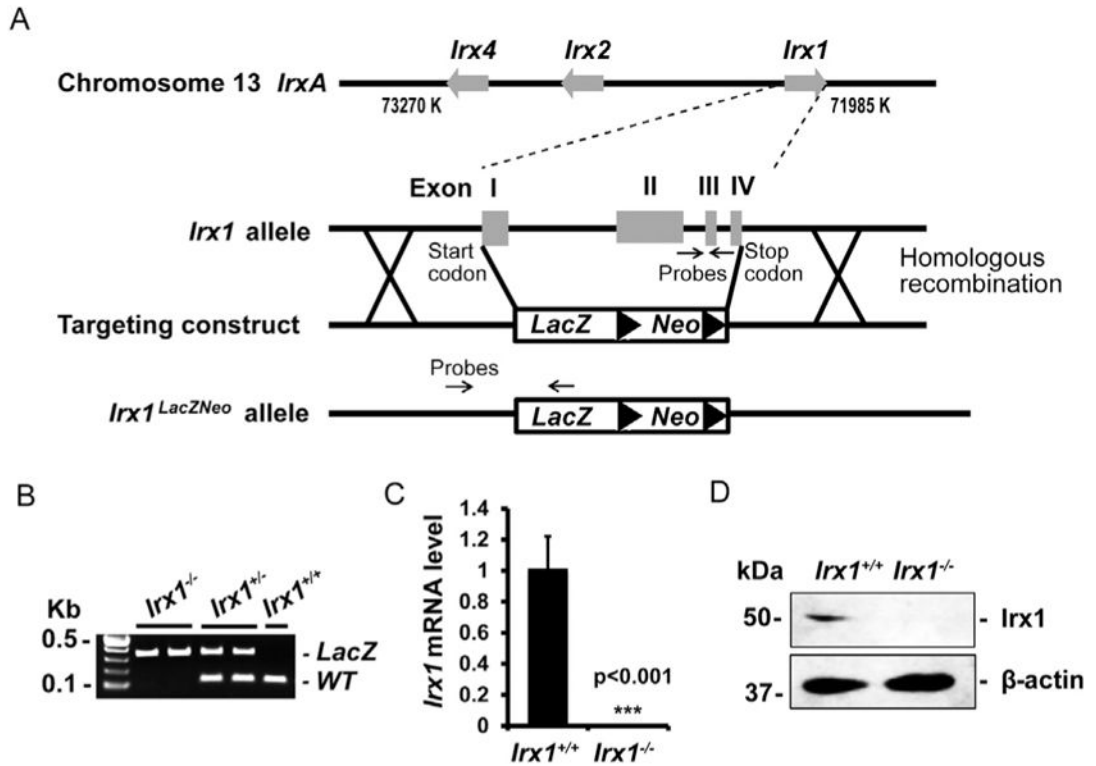


Fig. 1. Generation of the *Irx1* knockout mice

(A) Schematic diagram of *IrxA* cluster, *Irx1* allele, targeting construct and recombinant allele. The targeting construct carries a *LacZ* reporter gene and a neomycin resistance gene (*Neo*). The entire *Irx1* sequence from start codon to stop codon is replaced by *LacZ-Neo* in *Irx1* knockout mice. Probes position shows the sites of primers for genotyping. (B) RT-PCR result of *Irx1* genotyping strategy. *Irx1^{+/+}* mice only have a 106 bp *WT* band, *Irx1^{-/-}* mice only have a 400 bp *LacZ* band, *Irx1^{+/-}* mice have both of the bands. (C) qRT-PCR analysis of *Irx1* mRNA level in P0 *Irx1^{+/+}* and *Irx1^{-/-}* lung tissue. (D) Western blot result shows *Irx1* protein is ablated in *Irx1^{-/-}* lung tissue. ***, $p < 0.001$.

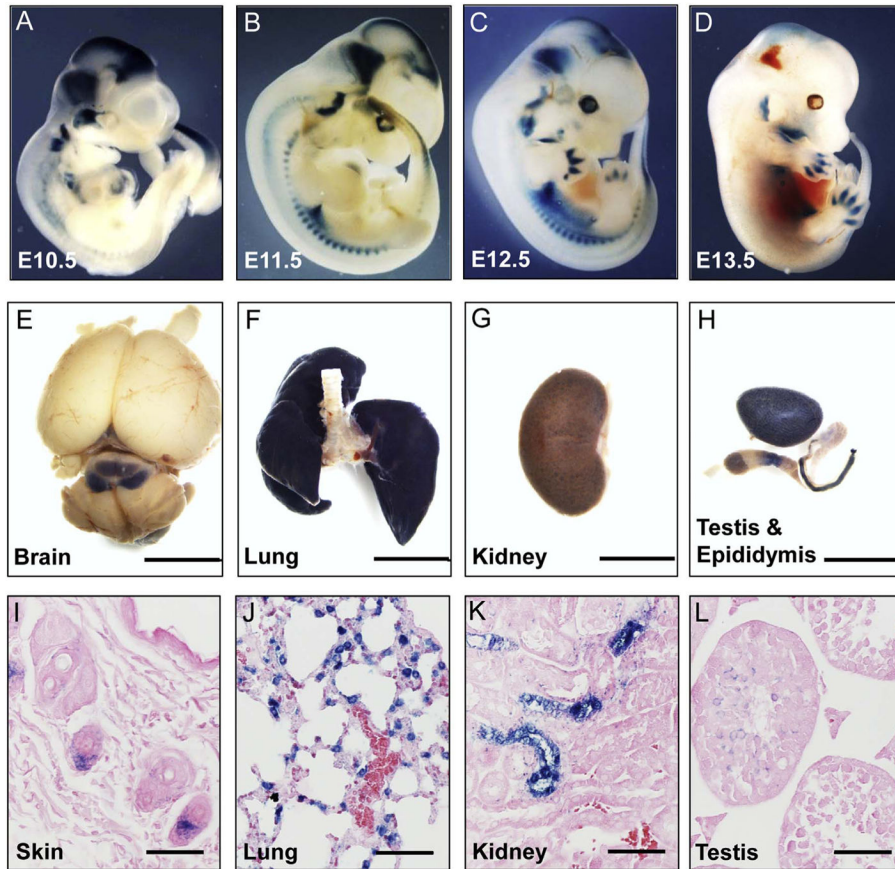


Fig. 2. Expression pattern of *Irx1* in mice

(A–D) Whole mount X-gal staining of *Irx1*^{+/-} embryos at E10.5, E11.5, E12.5 and E13.5. (E–H) Whole mount X-gal staining of brain, lung, kidney, testis and epididymis in *Irx1*^{+/-} adult mice at P30. Scale bar: 5 mm. (I–L) Eosin staining of PFA-fixed paraffin-embedded sections from X-gal-stained adult organs of skin, lung, kidney and testis. Scale bar: 50 μ m.

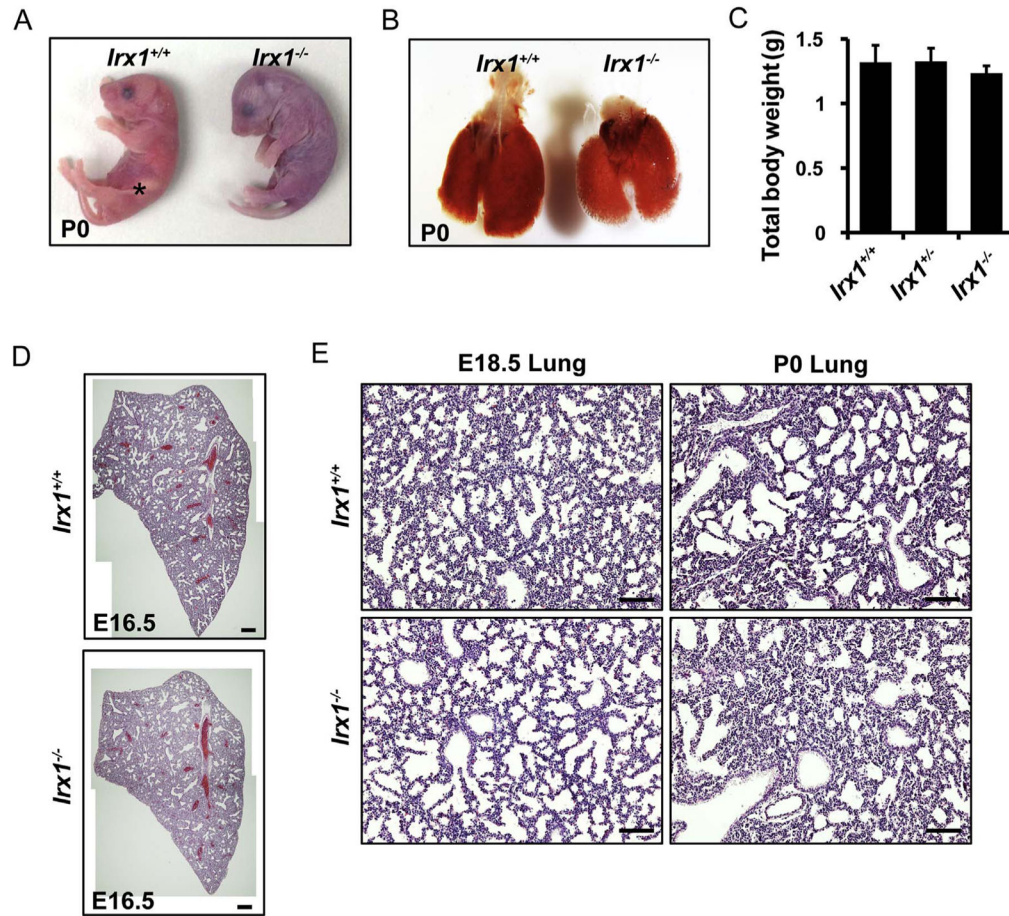


Fig. 4. *Irx1* ablation leads to neonatal lethality and lung defects

(A) Representative image of *Irx1^{+/+}* and *Irx1^{-/-}* pups right after birth. *Irx1^{+/+}* pup has milk in stomach (indicated by asterisk). (B) Representative image of lung from *Irx1^{+/+}* and *Irx1^{-/-}* mice at P0. The lung from *Irx1^{-/-}* mouse is smaller compared to the lung *Irx1^{+/+}* mouse. (C) Total body weight of *Irx1* new born pups. (D) Representative hematoxylin & eosin staining images of the left lung from E16.5 embryos. Histological structure of the lung from *Irx1^{-/-}* embryos is similar to the lung from *Irx1^{+/+}* embryos. (E) Histological analysis of lung from E18.5 and P0 *Irx1^{+/+}* and *Irx1^{-/-}* mice. E18.5 and P0 embryos were fixed and the left lung was used for analysis. Scale bar: 200 μ m (D), 50 μ m (E).

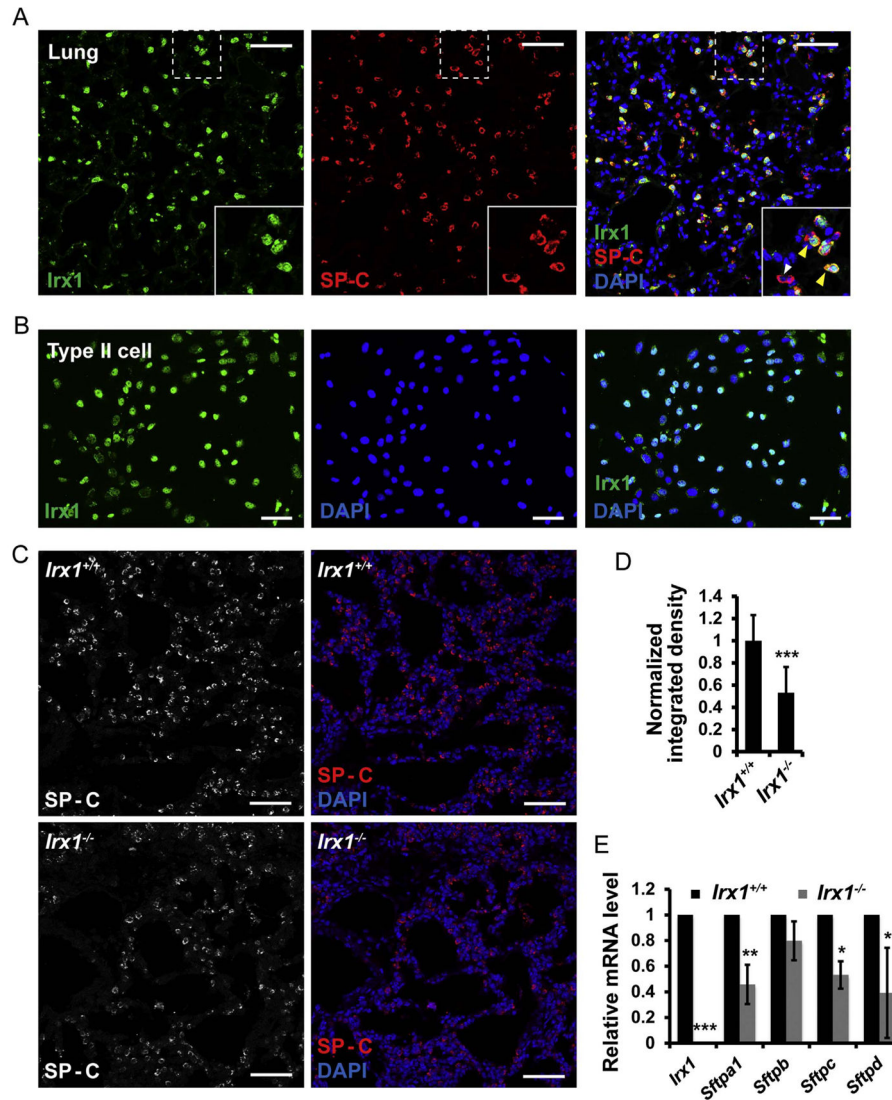


Fig. 5. *Irx1* marks alveolar type II epithelial cells and regulates surfactant proteins expression (A) Immunostaining of *Irx1* and SP-C in adult lung. Yellow arrows show *Irx1*⁺ cells are co-stained with SP-C. The white arrow shows only SP-C expression. (B) Immunostaining of *Irx1* in AEC2 cell line from rats. All cells are stained with *Irx1* antibody and 4'-6-diamidino-2-phenylindole (DAPI). (C) Bar chart shows the fluorescent density of SP-C in *Irx1^{+/+}* and *Irx1^{-/-}* left lungs at P0 stage. $p = 0.00012$. (D) Bar chart shows the percentage of SP-C⁺ cells in *Irx1^{+/+}* and *Irx1^{-/-}* left lungs at P0 stage. (E) Quantitative RT-PCR analysis of *Irx1* and surfactant proteins mRNA level in the left lung of E18.5 stage embryos. $n = 6$, *, $p < 0.05$; **, $0.01 < p < 0.05$; ***, $p < 0.001$. Scale bar: 50 μm . (For interpretation of the references to color in this figure legend, the reader is referred to the web version of this article).

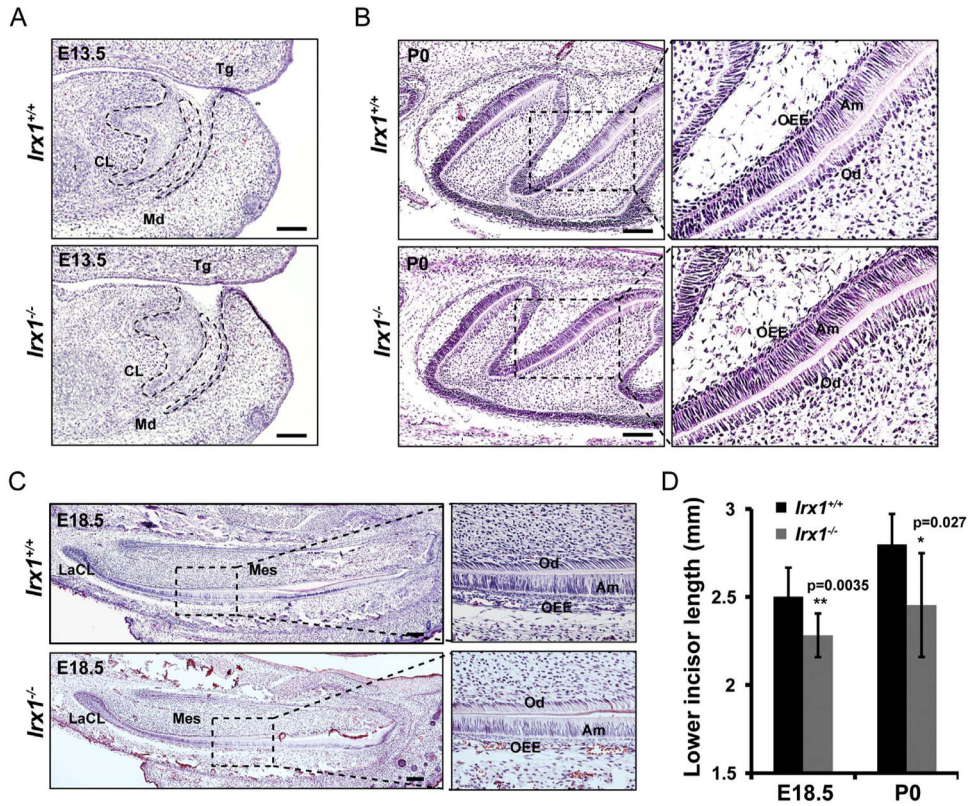


Fig. 6. Tooth growth is reduced in *Irx1*^{-/-} embryos

(A) Representative images of hematoxylin & eosin staining in E13.5 lower incisors. The invagination of dental development is delayed in *Irx1*^{-/-} lower incisors. CL, cervical loop; Tg, tongue; Md, mandible. (B, C) Representative images of hematoxylin & eosin staining in molars (P0) and lower incisors (E18.5) in *Irx1*^{+/+} and *Irx1*^{-/-} mice. OEE, outer enamel epithelium; Am, ameloblasts; Od, odontoblasts; Mes, mesenchyme; LaCL, labial cervical loop. (D) Bar chart shows statistical analysis of lower incisor length in E18.5 and P0 *Irx1*^{+/+} and *Irx1*^{-/-} mice. Lower incisors in *Irx1*^{-/-} are shorter respectively. Mean \pm s.e.m; N = 6, p values are shown in bar chart. Scale bar: 100 μ m.

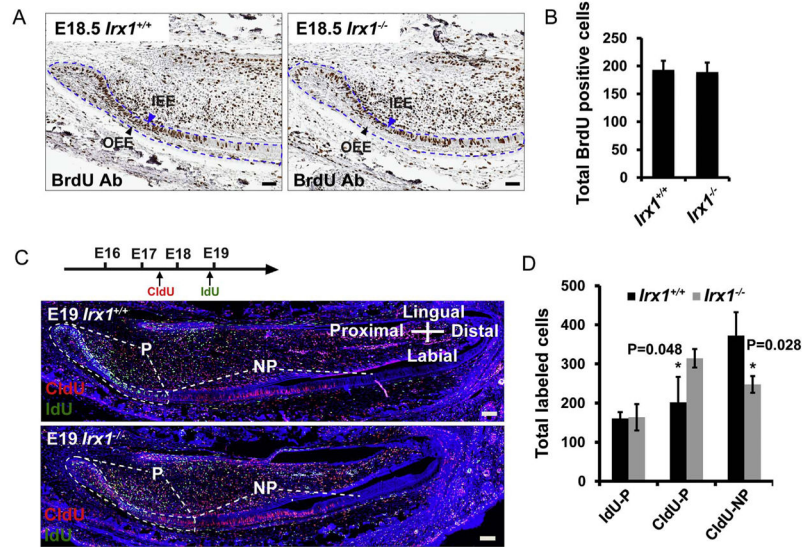


Fig. 7. Epithelial cell differentiation is decreased in *Irx1*^{-/-} mice

(A) BrdU immunohistochemistry staining of E18.5 lower incisors. BrdU was injected into pregnant female 2 h before harvesting. Representative images show dental epithelial cells (dashed outline) at the cervical loop region marked with BrdU signals. Blue arrows show that IEE cells are labeled with BrdU signals; black arrows show that OEE cells are not labeled with BrdU signals. (B) Bar chart shows total cell number of BrdU positive cells in the dashed outline region. (C) CldU and IdU double immunofluorescence staining at E19. CldU (36 h pre-harvest) and IdU (2 h pre-harvest) were injected into pregnant female before harvesting at E19 (see diagram). Dashed lines show the proliferation zone of dental epithelial layers including the labial cervical loop of the lower incisors (P). Images were generated by Zeiss 700 with multiple horizons. Notice there is horizon shift in images. (D) Bar chart shows total IdU or CldU positive cell number in different regions of the dental epithelial cell layers. IdU-P, IdU positive cells of the labial cervical loop and transient amplifying cells; CldU-P, CldU positive cells of the labial cervical loop and transient amplifying cells; CldU-NP, CldU positive cells of the dental epithelial cells outside of the labial cervical loop. Scale bar: 100 μ m; n = 3; *, p < 0.05. (For interpretation of the references to color in this figure legend, the reader is referred to the web version of this article).

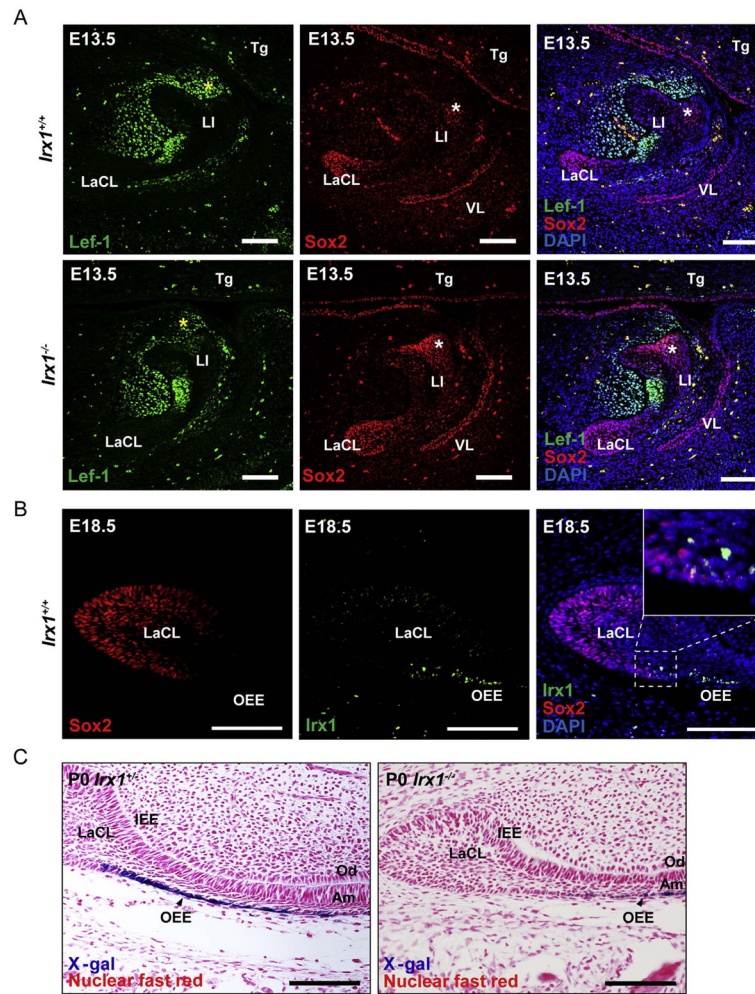


Fig. 8. *Irx1* regulates the number and partitioning of Lef-1+ and Sox2+ cells during incisor development

(A) Double immunofluorescence staining of Sox2 and Lef1 in cap stage lower incisors. Sox2 positive cell distribution is altered in *Irx1*^{-/-} lower incisors. Yellow asterisks show Lef-1 expression in lingual dental mesenchyme; white asterisks show *Irx1* expression within Sox2+ cells. LI, lower incisor; LaCL, labial cervical loop; VL, vestibular lamina (B) Double immunofluorescence staining shows *Irx1* and Sox2 are differentially expressed in the dental epithelium of the lower incisor. Enlarged panel shows few cells co-expressing both *Irx1* and Sox2. (C) X-gal & nuclear fast red staining of lower incisors from P0 *Irx1*^{+/+} and *Irx1*^{-/-} mice. Representative images show there are less OEE (X-gal positive) cells of *Irx1*^{-/-} lower incisor. OEE, outer enamel epithelium; CL, cervical loop; IEE, inner enamel epithelium; OD, odontoblasts; Am, ameloblasts; Tg, tongue. Scale bar: 100 μ m. (For interpretation of the references to color in this figure legend, the reader is referred to the web version of this article).

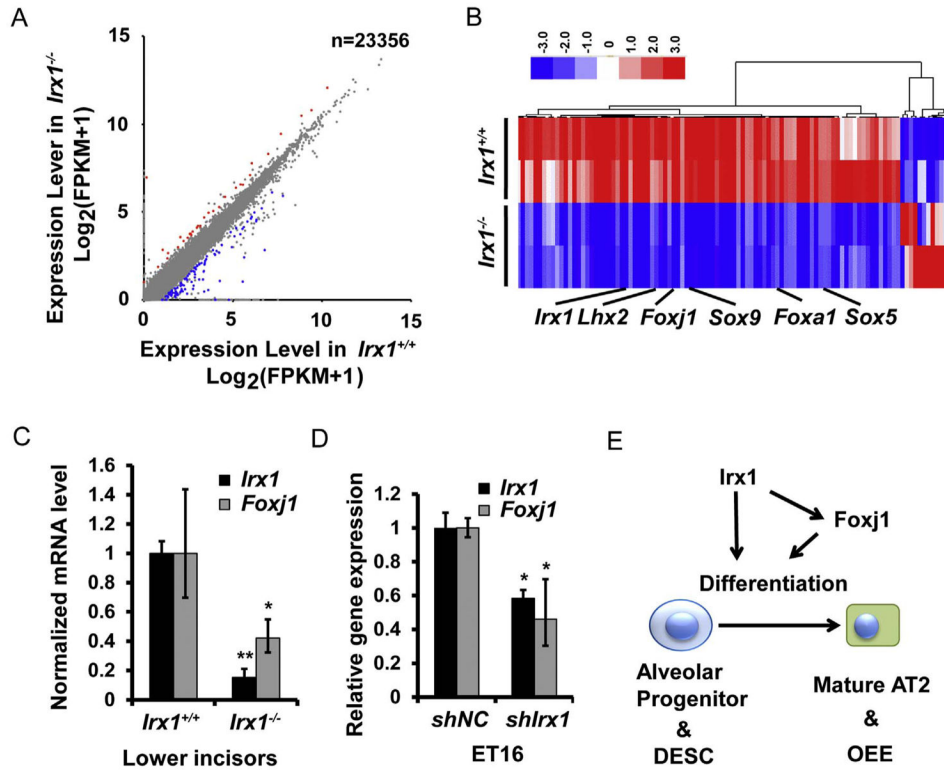


Fig. 9. *Irx1* regulates differentiation-related gene expression including *Foxj1*

(A) Scatter plot shows the results of RNA-seq analysis in E14.5 *Irx1*^{+/+} and *Irx1*^{-/-} mandible and maxilla. Blue dots represent genes down-regulated in *Irx1*^{-/-} tissues; Red dots represent genes up-regulated in *Irx1*^{-/-} tissues. (B) Heat map shows genes significantly up-regulated or down-regulated in *Irx1*^{-/-} tissues generated from RNA-seq analysis. (C) Quantitative analysis of *Foxj1* expression in *Irx1*^{+/+} and *Irx1*^{-/-} lower incisors. Lower incisors from P0 mice were dissected and dental epithelial cells were used for gene expression analysis. *Foxj1* mRNA level from *Irx1*^{-/-} group is down-regulated as shown in the bar chart. (D) *Foxj1* expression was down-regulated in *Irx1* knockdown ET16 cells. (E) The working model of *Irx1* in mouse embryonic development. (For interpretation of the references to color in this figure legend, the reader is referred to the web version of this article).

Table 1

Genotypes of offspring from *Irx1*^{+/-} intercrosses. Embryos and new born pups were harvested from E12.5 embryonic stage to P1. Numbers in parenthesis indicate dead newborns.

Developmental stage	Genotype			Total
	+/+	+/-	-/-	
E12.5/E13.5	8	13	4	25
E14.5/E15.5	25	35	19	79
E16.5/E17.5	6	21	5	32
E18.5	13	25	14	52
P0	20	37	19 (4)	76
P1	13	28	0	41

Author Manuscript

Author Manuscript

Author Manuscript

Author Manuscript

Table 2

List of primers used for quantitative RT-PCR.

Gene	Forward primer (5'-3')	Reverse primer (5'-3')
<i>β-Actin</i>	CTCTTCCAGCCTTCCTTC	ATCTCCTTCTGCATCCTGTC
<i>Irx1</i>	ACACCTGACAGCACCACCA	GCAAAAGTAAAAGATGACCCC
<i>Stipal</i>	GAGAGATGTGTACCAGAGCCG	GTAGTGGAAGTCTCCAGGAGTC
<i>Stipb</i>	TTCAAGCCGTGATCCCAAG	CAGCAGTGCGTCTAGCAGG
<i>Stipc</i>	TCCTCGTTGTCGTGGTGATTG	GGAAAAGGTAGCGATGGTGTC
<i>Stipd</i>	CTCCCACTATCAGAAAGCTGC	CCCACATCTGTCATACTCAGGAA
<i>Foxj1</i>	ATCACTCTGTCGGCCATCTAC	GCAGGGTGGATGTGGACTG

Author Manuscript

Author Manuscript

Author Manuscript

Author Manuscript